

# Airbag-Based Crew Impact Attenuation Systems for the Orion Vehicle – Single Airbag Optimization

Anonymous MIT Students

*Department of Aeronautics and Astronautics, Massachusetts Institute of Technology, Cambridge, MA, 02139*

Airbag-based methods for crew impact attenuation have been highlighted as a potential means of easing the mass constraints currently affecting the design of the Orion Crew Exploration Vehicle. This paper focuses on both the single and multi- objective optimization of a simplified version of such a system using both gradient-based and heuristic methods. From this, it is found that for systems implemented with pressure relief valves, the optimal design is one with the minimum geometry such that bottoming-out does not occur. Moreover, maintaining this condition while varying the burst pressure of the valve was found to correspond to moving along points on the Pareto front of impact attenuation performance and system mass.

## I. Introduction

Traditionally, manned Earth reentry vehicles have used rigid structures supported by shock-absorber type systems to protect astronauts from the impact loads incurred upon landing. These systems have consistently proven to be reliable and capable for their intended function on vehicles of the past. However, the advantages of their impact attenuation performance over their mass penalty have been questioned for more capable and inherently complex spacecraft systems. This is particularly the case for the recently redirected Orion Crew Exploration Vehicle program, where the mass budget was constantly under strain due to highly demanding performance requirements. In response to this, airbag-based systems have been identified as a potential alternative to this concept, as shown in Figure 1.

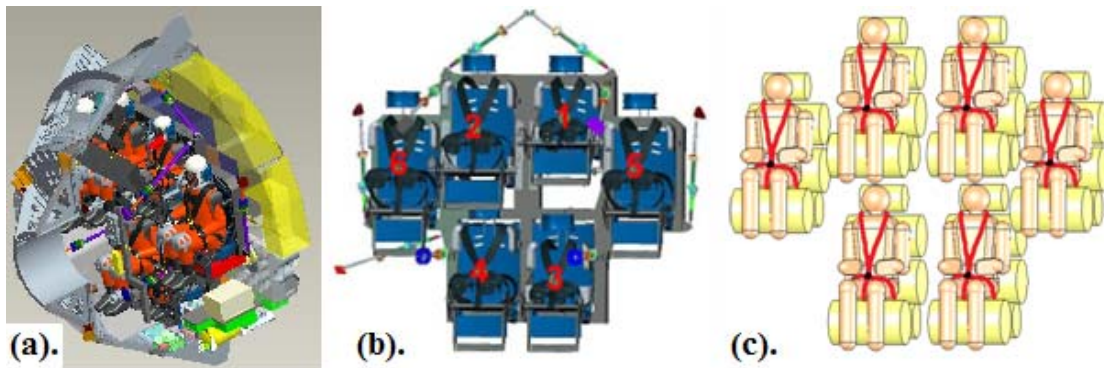


Figure 1– (a). Orion CEV Baseline Configuration (b). Orion’s Baseline Crew Impact Attenuation System (c). Airbag-Based Crew Impact Attenuation System Concept to be Investigated

The main advantage of such a configuration is its significantly lower mass relative to traditional crew impact attenuation system (CIAS) designs, whilst having potentially comparable or even improved performance. An additional benefit includes the ability of airbag systems to be deflated and stowed away, hence providing additional in-cabin volume once the spacecraft is in orbit. Initial estimates have found that compared to the baseline design of the Orion CEV, these savings equate to a potential 36% reduction in CIAS mass without the crew, and an increase of 26% in in-orbit habitable volume<sup>1</sup>.

---

\* Graduate Research Assistant, Department of Aeronautics and Astronautics, Massachusetts Institute of Technology, Cambridge, MA, 02139, and AIAA Student Member

## II. System Modeling

Airbags attenuate impact loads by converting the kinetic energy of an impacting event into the potential energy of a compressed gas, and then venting this gas to remove energy from the system. In order to model this phenomenon, several disciplines and their interactions need to be captured. These include thermodynamics, fluid mechanics, and structural dynamics.

For the current study, these disciplines were combined to model the impact dynamics of a single airbag, rather than that of a multi-airbag system (see Figure 2). This decision was made after a failed attempt at modeling the dynamics of a multi-airbag system in a robust and reliable manner within the time constraints imposed on this study. Thus, it is intended for the framework developed in this study to be incorporated with a multi-airbag model once it is developed in the future.

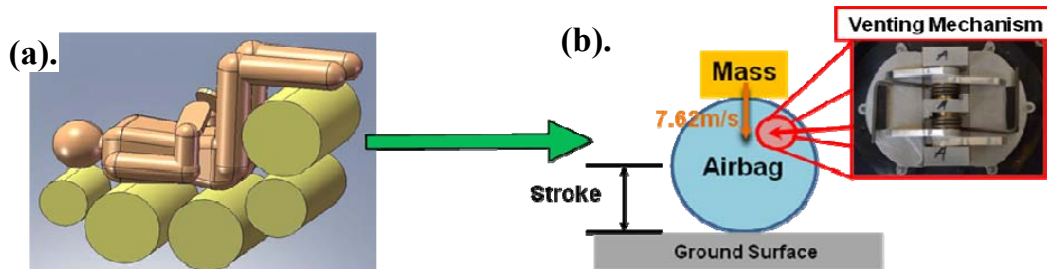


**Figure 2 – (a). Original Airbag-based Crew Impact Attenuation System Concept (b). Simplified System Model (Inset – Flapper-type Pressure Relief Valve)**

As can be seen in Figure 2, the system modeled consists of a cylindrically shaped fabric bladder, filled with a gas at a given pressure and loaded with a test mass. In addition, the concept also consists of a venting mechanism, which facilitates the expulsion of gas from the system. Currently, the design of this venting mechanism is fixed to be a flapper-type pressure relief valve of fixed venting area, but with adjustable burst pressure, as shown in Figure 2(b). Also fixed are the operating medium, being air, the impact velocity of 7.62m/s, which corresponds to the nominal impact velocity of the Orion vehicle, and the environmental parameters of gravitational acceleration and standard atmospheric pressure. These are summarized below in Table 1.

**Table 1 – System Fixed Parameters**

Fixed Parameter	Value	Comments
Airbag Geometry	Cylindrical	Selected for ease of manufacture
Venting Mechanism Concept	Flapper-type pressure relief valve	Design fixed before this study
Venting Area	Equivalent to a 2 x Ø2" area	Fixed before this study. May be revisited as a design variable in the future
Operating Medium ( $\gamma$ )	Air (1.4)	Compatible with spacecraft cabin atmosphere
Impact Velocity	7.62m/s	Nominal impact velocity of Orion CEV
Gravitational Acceleration	9.81m/s <sup>2</sup>	Landing on Earth's surface
Atmospheric Pressure	101.325kPa	Assumed landing in standard atmospheric conditions
Test Mass	2.5kg	Corresponds to mass of occupant head. This will be the test condition for this study

Based on the information given in Table 1, the design variables can be defined as the remaining values required to characterize the impact dynamics of the system. These, along with their bounds are given in Table 2.

**Table 2 – System Design Variables**

Design Variable	Range	Comments
Radius [R] (m)	$0.1 \leq R \leq 0.5$	Lower geometry bounds correspond to geometric requirements of the human body, whilst upper bounds correspond to space constraints within the Orion CEV cabin
Length [L] (m)	$0.3 \leq L \leq 0.85$	
Inflation Pressure [ $P_{bagI}$ ] (Pa)	$P_{bagI} \geq 101325$	Airbag internal pressure must be $\geq$ atmospheric pressure in order to maintain its shape
Valve Burst Pressure [ $\Delta P_{burst}$ ] (Pa)	$\Delta P_{burst} > 0$	Measured as pressure in addition to inflation pressure. This value must be positive to allow for the airbag to inflate initially (ie. initial pressure < pressure at burst)

In regards to the system metrics, impact attenuation capability and mass have been selected as the basis for the optimization framework developed. Here, impact attenuation capability is measured by a metric known as the Brinkley Direct Response Index. This index measures the risk of injury to an occupant given a measured acceleration profile by comparing the output of a dynamics model of the human body, with limiting values representing varying levels of risk to injury. In order for its performance to be deemed acceptable, NASA requires impact attenuation systems to have a nominally low level of risk to injury in all directions, as defined in Table 3.

**Table 3 – Brinkley Direct Response Index Limits (Obtained from REF[2])**

Direct Response Level	X		Y		Z	
	$DR_X < 0$	$DR_X > 0$	$DR_Y < 0$	$DR_Y > 0$	$DR_Z < 0$	$DR_Z > 0$
Very Low (Nominal)	-22.4	31	-11.8	11.8	-11	13.1
Low (Off-Nominal)	-28	35	-14	14	-13.4	15.2
Moderate	-35	40	-17	17	-16.5	18
High Risk	-46	46	-22	22	-20.4	22.4

With this, the system fixed parameters, design variables, and metrics were incorporated into a dynamics model based on the same code used for the preliminary design of the Mars Pathfinder airbag system. Figure 3 presents a high level N<sup>2</sup> diagram of this model.

An important point which is demonstrated by Figure 3 is that the calculation of the Brinkley Index requires a time history, and consequently for the set of governing equations to be integrated over a time horizon. Specifically, a Brinkley Index time history is calculated and the maximum magnitude is recorded as corresponding to the highest risk to injury during the impacting event. This in turn results in each function evaluation taking approximately 3 to 5 seconds to complete, which can be significant when implemented

within a multidisciplinary optimization scheme.

Additionally, this model was validated against a baseline case presented in REF[3]. Here, this case consisted of an airbag structure made of three 0.456m radius spheres combined in a triangular manner, impacting at 20.67m/s on the Earth’s surface. Figure 4 presents a comparison in velocity and acceleration time histories.

As can be seen in Figure 4, the dynamic history results generated by the developed system model are very similar to those outputted by the baseline model, with a maximum error of 2 to 3% between the two. This in turn provides enough confidence in the accuracy of the model for implementation into an optimization framework, which will be discussed in the next section.

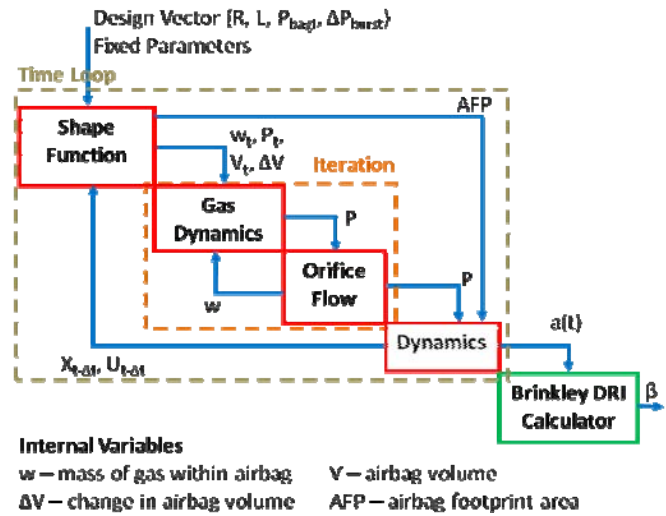


**Figure 3 - N<sup>2</sup> Diagram of Single Airbag Model.** The various disciplines involved correspond roughly to the following function blocks: Shape Function – Fluid Dynamics, Gas Dynamics – Fluid Dynamics & Thermodynamics, Orifice Flow – Fluid Dynamics, Dynamics – Structural Dynamics

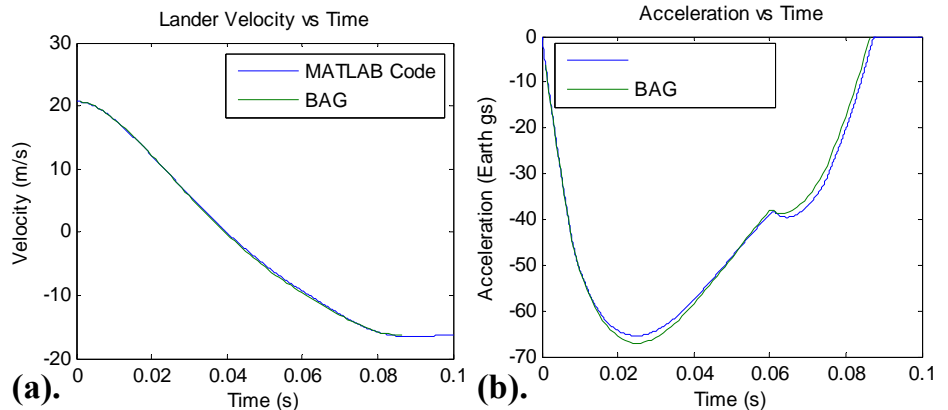


**Figure 4 – Validation of System Model (a). Velocity (b). Acceleration**

### III. System Optimization

The optimization of the single airbag system can be divided into two components. The first component consists of a single objective optimization, where the focus is on minimizing Brinkley DRI. Whilst the second component involves a multi-objective optimization, where minimizing the Brinkley DRI and minimizing the total system mass are the dual objectives of the optimization.

The single objective optimization started with a Design of Experiments (DOE) study, followed by a gradient-based optimization method, and finally a heuristic optimization method. Specifically, the DOE was performed using an orthogonal array, with the optimal result being selected as the starting point for the gradient based method. Sequential Quadratic Programming (SQP) was then chosen to perform the gradient-based optimization, and Simulated Annealing (SA) method was chosen to perform the heuristic-based optimization. Following this, a multi-objective optimization was performed using a full factorial expansion method. Each of these methods will be discussed in the following sections.

#### A. Single Objective Optimization

As was previously mentioned, the Brinkley index was selected as the objective for the single objective optimization. Based on the information provided in Section 2, this problem can be formulated as follows:

$$\begin{aligned} &\text{Minimize } \beta = \text{Maximum injury risk} = \text{Maximum Brinkley Direct Response Index} \\ &\text{Subject to:} \\ &\quad 0.1 \leq R \leq 0.5 \quad [\text{m}] \\ &\quad 0.3 \leq L \leq 0.85 \quad [\text{m}] \\ &\quad P_{\text{bagI}} \geq 101325 \quad [\text{Pa}] \\ &\quad \Delta P_{\text{burst}} \geq 0 \quad [\text{Pa}] \end{aligned}$$

It is interesting to note that the only constraints present within this problem correspond to bounds on the design variables, as presented in Table 2. This is due to the fact that only a single-airbag model is being studied. For a multi-airbag system however, additional constraints would be required to capture the interactions between each of the airbags. An example of this is that the sum of the airbag diameters (ie. the total length of the system), would have to be within some range of the sitting height of the occupant.

Hence with this formulation now composed, a series of methods was used to study trends in the problem solution. These are expanded upon in the proceeding sections.

#### 1. Design of Experiments

The Design of Experiments method was used to perform a preliminary sampling of the design space, thus allowing for rough trends in the objective with respect to the design variables to be observed. Here, the factors were chosen to correspond to each of the design variables in the problem, being the: airbag radius, length, bag pressure and burst pressure. Three levels of values for each factor were selected to represent an even spread across the design domain. These are shown in the following table:

**Table 4 – Factors and Levels for the Design of Experiments**

Factor	Level 1	Level 2	Level 3
<b>A: Radius (m)</b>	0.2	0.3	0.4
<b>B: Length (m)</b>	0.3	0.5	0.7
<b>C: P<sub>bagI</sub> (atm)</b>	1.0	1.1	1.2
<b>D: ΔP<sub>burst</sub> (kPa)</b>	8	12	16

For this study, the orthogonal arrays method was used to sample the design space. For an experiment with four factors and three levels for each factor, a full factorial design would require  $3^4$  or 81 experiments. By using the orthogonal arrays method, the number of required experiments is reduced from 81 to 9. Although the orthogonal arrays design is a subset of the full-factorial experiment, the design of the experiments is efficient and balanced.

The experiment design matrix and the resulting Brinkley DRI is listed as follows:

**Table 5 – Design of Experiments Results**

	<b>A: Radius</b>	<b>B: Length</b>	<b>C: P<sub>bag1</sub></b>	<b>D: dP<sub>burst</sub></b>	<b>DRI</b>
<b>Experiment 1</b>	A1: 0.2	B1: 0.3	C1: 1.0	D1: 8	3.7446
<b>Experiment 2</b>	A1: 0.2	B2: 0.5	C2: 1.1	D2: 12	4.6524
<b>Experiment 3</b>	A1: 0.2	B3: 0.7	C3: 1.2	D3: 16	5.5905
<b>Experiment 4</b>	A2: 0.3	B1: 0.3	C2: 1.1	D3: 16	4.4509
<b>Experiment 5</b>	A2: 0.3	B2: 0.5	C3: 1.2	D1: 8	5.3566
<b>Experiment 6</b>	A2: 0.3	B3: 0.7	C1: 1.0	D2: 12	5.8517
<b>Experiment 7</b>	A3: 0.4	B1: 0.3	C3: 1.2	D2: 12	4.7864
<b>Experiment 8</b>	A3: 0.4	B2: 0.5	C1: 1.0	D3: 16	5.6779
<b>Experiment 9</b>	A3: 0.4	B3: 0.7	C2: 1.1	D1: 8	5.8278

To calculate the effect of each design factor and level, the overall mean of the Brinkley DRI,  $m$ , is first calculated. Then the main effect of each design factor and level is calculated by averaging the Brinkley DRI values when that factor and value is fixed. Eg:

$$m_{A1} = \frac{DRI_1 + DRI_2 + DRI_3}{3} \tag{1}$$

The main effect of a level of a factor, in this case A1, is then calculated by:

$$\text{Effect of radius level A1} = m_{A1} - m \tag{2}$$

Repeating the same procedure to find the effects of other factors and levels, the effects of all the factors and levels can be obtained. These are shown in Table 6.

From the results, it can be seen that A1, B1, C3 and D3 have the largest effect on the mean Brinkley Index for the corresponding design factor. In addition, since the objective is to minimize Brinkley DRI, a starting point of (A1 B1 C2 D1) will be selected. This corresponds to:

$$x_0 = (0.2m, 0.3m, 1.1atm, 8kPa)$$

An interesting point to note is that the results of this exercise indicate that smaller geometries lead to lower Brinkley DRI values and hence improved impact attenuation performance, which seems unintuitive. As will be seen in the following sections, this trend was consistently observed with all optimization schemes used. Consequently, an investigation was performed in an attempt to explain this phenomenon. This is discussed in Section III.A.4.

**Table 6 – Main Effect of Design Variables**

Main effect of A1	-0.44
Main effect of A2	0.12
Main effect of A3	0.33
Main effect of B1	-0.78
Main effect of B2	0.12
Main effect of B3	0.65
Main effect of C1	-0.01
Main effect of C2	-0.13
Main effect of C3	0.14
Main effect of D1	-0.13
Main effect of D2	-0.01
Main effect of D3	0.14

## 2. Sequential Quadratic Programming

For the gradient-based optimization, a Sequential Quadratic Programming (SQP) method was chosen. This selection is based on the fact that for the single airbag system, no simple analytical expression is available to express the objective function; and is due to the fact that it arises from the solution to a highly non-linear set of numerically solved equations. Because SQP uses an approximation to the Hessian rather than requiring an analytical form of one, the method lends itself naturally to this problem. In addition, the fact that SQP is designed to inherently handle constraints allows it to easily accommodate the bound constraints of this problem.

### Unscaled Case

As was mentioned in the previous section, the result of the Design of Experiments was used as an initial guess for an unscaled run of the SQP. Figure 5 shows the iteration time history and solution of this run.

Here, it can be seen that like the result of the Design of Experiments, the geometric component of the solution hits the lower bounds. The reasons behind this will be explored in Section III.A.4. Contrastingly, a change in the burst pressure resulted in a significant reduction in the Brinkley Index.

#### Scaled Case

In an attempt to obtain a better gradient-based solution, the SQP scheme was rerun with a scaled design vector. This vector was determined by calculating the Hessian of the system at the optimal solution, which in turn, was obtained with the use of a second order accurate finite difference approximation to the second derivative. This is given as follows:

$$f''(x) \approx \frac{f(x+\Delta x) - 2f(x) + f(x-\Delta x)}{\Delta x^2} \quad (3)$$

Here, the value of  $\Delta x$  was chosen to be  $\Delta x = 1 \times 10^{-8}$ , based on enforcing the rounding error to be comparable to the truncation error. With this, the diagonal terms of the Hessian were calculated to be approximately:

$$\begin{aligned} H_{11} &= 6.671 \times 10^{12}, H_{22} = 1.004 \times 10^{12}, \\ H_{33} &= -61733220, H_{44} = 0 \end{aligned} \quad (4)$$

As can be seen from this result, three of the four diagonal terms are in need of scaling. The magnitude of scaling required can be calculated by attempting to make the order of the Hessian terms equal to one. Thus, the scaling terms can be calculated using the following relationship:

$$ScalingFactor = O(H_{ii}^{-0.5}) \quad (5)$$

Therefore:

$$Scaling\ Factor = L = \begin{bmatrix} 10^{-7} & & & \\ & 10^{-7} & & \\ & & 10^{-4} & \\ & & & 1 \end{bmatrix} \quad (6)$$

With this, the SQP scheme was re-run, yielding the results given in Figure 6.

Again, it can be seen that the overall impact attenuation performance of the system has improved after this run. Also observed is the fact that the consistent trend towards smaller geometries has once more occurred. This will be investigated in Section III.A.4.

### 3. Simulated Annealing

In addition to gradient-based methods, heuristic techniques were also used to solve the single-airbag single objective optimization problem. This was due to the fact that the large search space and complex interactions between the non-linear governing system equations results in the potential for many local optima to occur. Because of their inherent randomness, heuristic techniques are capable of identifying the global optimum of the problem under these conditions.

Here a Simulated Annealing (SA) method was used, primarily due to its requirement for less function evaluations when compared to other methods. A comparison with the genetic algorithm revealed that for the problem studied here, between 20 and 60 function evaluations per generation were required. Contrastingly, for an SA method under an exponential cooling schedule, approximately ten temperature states of evaluation would be required. Setting the number of rearrangements to 50 at each temperature state would still require much less calculation time.

As was previously mentioned, the optimal values obtained from SQP were selected as the starting point for the Simulated Annealing scheme; with the upper and lower bounds for the perturbation in each design variable chosen to be

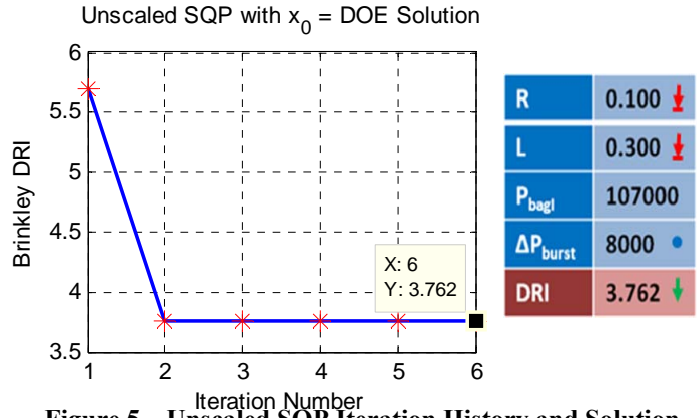


Figure 5 – Unscaled SQP Iteration History and Solution

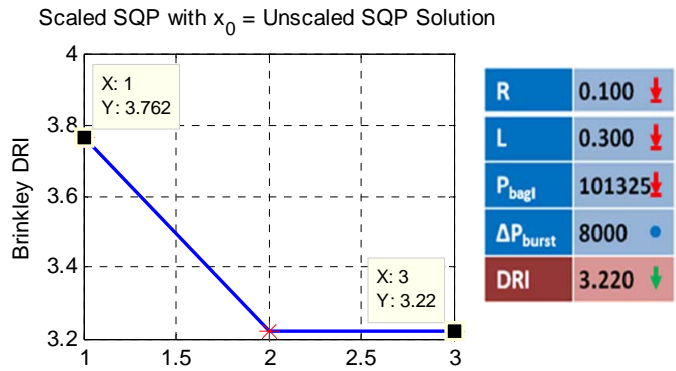


Figure 6 – Scaled SQP Iteration History and Solution

the same as those previously specified. Here, the major parameters for the system were selected based on previous experimentation with various combinations of settings. The final parameters used are summarized in Table 7 below:

**Table 7 – Simulated Annealing Tuning Parameters**

SA Parameters	Values	Rationale
To - initial system temperature	500	Guarantees a good initial sampling of the design space
Cooling Schedule	Exponential	Proven to be effective in terms of the optimality of the final result and computation time
dT Temperature Increment	0.1	Experimentation showed that this value was appropriate for the problem at hand
Equilibrium Condition	20	Ensures that enough configurations are evaluated before moving to the next temperature state

With these final tuning parameters, the results presented in Figure 7 were obtained.

Observing the SA iteration history, it can be seen that the algorithm first samples through different parts of the design space at the initial temperature state. As the temperature reduces, the scheme behaves more like a gradient based method and concentrates on a specific region of the design space. The optimal solutions are found near the termination of the algorithm.

With respect to the optimal solution obtained, it is interesting to note that unlike the gradient based schemes, none of the design variable bounds have been hit. This is the case even with an improved Brinkley Index. The reason for this behavior is explored and explained in Section III.A.4.

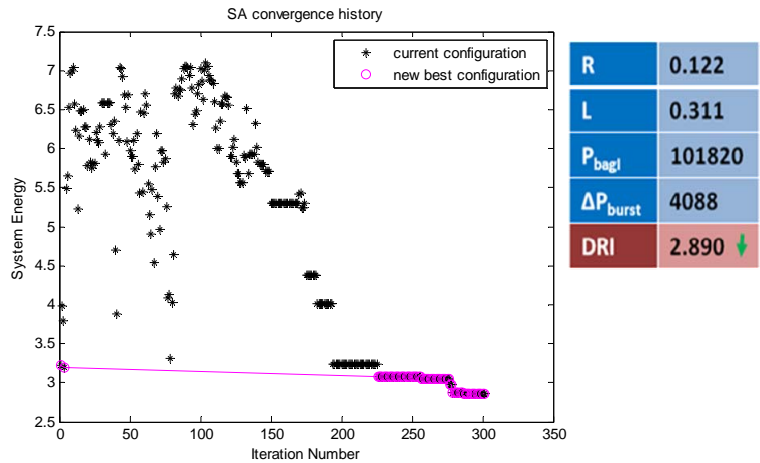


**Figure 7- Simulate Annealing Iteration History and Solution**

#### 4. Result Analysis

In this section, the trends in the results observed in the various single objective optimization runs will be analyzed. Specifically, the following will be investigated:

- The unintuitive trend towards a smaller airbag geometry for improved Brinkley Direct Response Index
- The fact that the simulated annealing analysis yielded a result with an improved Brinkley Index but without hitting the lower bounds of the design variables; as was observed with all previous optimization cases; and
- The sensitivities within the system

##### Correlation between Smaller Airbag Geometries and Improved Brinkley Index

Throughout the single objective optimization analysis, it was continually observed that the optimal solution tended toward the lower bound of the geometric design variables, indicating that a smaller airbag is preferable for impact attenuation. This counter-intuitive observation can be explained by comparing the orifice opening area time histories between two differently sized airbags, as shown in Figure 8.

Here, it can be seen that under the same impact conditions, the smaller airbag maintains a higher pressure over a longer period of time, which results in the pressure relief valve remaining open for a longer time period. Since the system reduces the energy from the impacting object by venting gas from the system, a longer time for gas release results in a better impact attenuation performance.

A succinct explanation for the effect of the orifice area arises from the fundamental energy conversions governing airbag impact attenuation. That is, the kinetic energy of the impacting system is converted into the internal energy of the airbag gas, which is in turn removed from the system as the airbag vents this gas. Because the amount of energy removed is directly related to the amount of gas released from the system, the geometry and opening duration of the orifice are critical factors.

However, it should be noted that there are limiting factors to how small the airbag geometry can feasibly be – one of which, being the amount of physical stroke available to damp the impacting system. Hence there appears to be two opposing factors which influence the direction in which the size of the optimal airbag should move. One which drives the system towards lower geometries to maximize the amount of time over which the venting orifice remains open, thereby allowing for more energy to be attenuated from the system; and one which pushes towards increasing the system geometry to avoid bottoming-out (where the occupant comes into direct contact with the ground). Based on these observations, it can be concluded that the optimum geometry would be one which minimizes the geometry such that bottoming-out does not occur. Further investigation indicated that the accuracy of the prediction of this geometry is directly influenced by the accuracy of the prediction of this geometry is directly influenced by the accuracy of the airbag shape function. That is, the function which predicts the geometry of the airbag as it is compressed during an impacting event. Because the shape function used was modified from that of the original Mars Pathfinder code to accommodate the problem at hand, there is currently low confidence the ability of the current model to predict the optimal airbag size. It is intended for this to be rectified in future studies via comparison with empirical data currently being obtained as part of the greater research behind this project.

The Simulated Annealing Solution Not Lying at the Lower Bounds of the Geometric Variables

In Section III.A.3, it was found that the result from the Simulated Annealing analysis had improved upon that of the gradient based methods. One unexpected observation made however, when the SA optimal was reached, the geometric variables did not hit their lower boundaries, as had been consistently observed earlier. To further investigate the reason for this, the design space was further examined. It became apparent that this phenomenon was related to how each scheme interpreted the design space. Shown below, are the Brinkley DRI indexes of the design space plotted over a coarse grid and a fine grid:

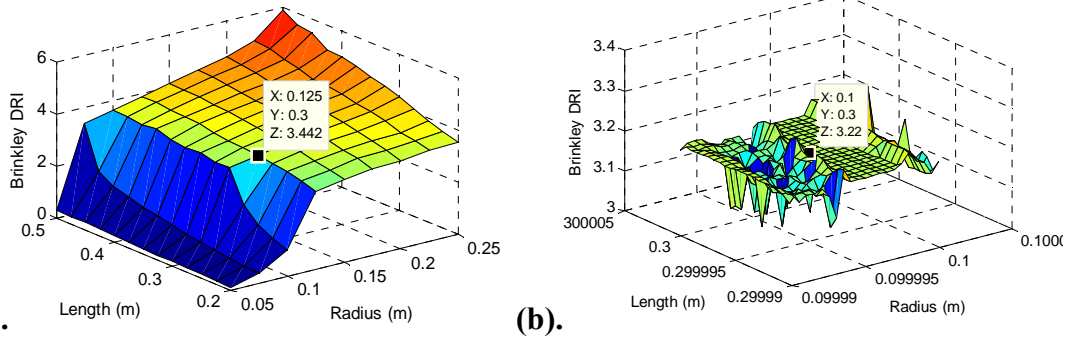


**Figure 9 – Brinkley DRI Space Plotted at (a). Coarse Resolution  $\Delta x = 0.025$  (b). Fine Resolution  $\Delta x = 10^{-6}$**

Here, it can be observed that under different resolutions, the design space has varying levels of noise. This is a result of the manner in which the Brinkley Index is calculated – that is, by integrating over a time horizon to obtain dynamic time histories, and then by calculating the maximum Brinkley DRI value from this.

With this finding, the discrepancy in the trends obtained between the SQP and SA methods can be explained by the fact that the step sizes used by SQP to step across the design space, were large enough to avoid the low amplitude high frequency noise spikes. This resulted in it following gradients measured over longer spatial steps towards the lower bounds. Contrastingly the stochastic nature of the SA scheme allowed it to better sample within the noisy regions of the design space, thus enabling it to find better solutions.

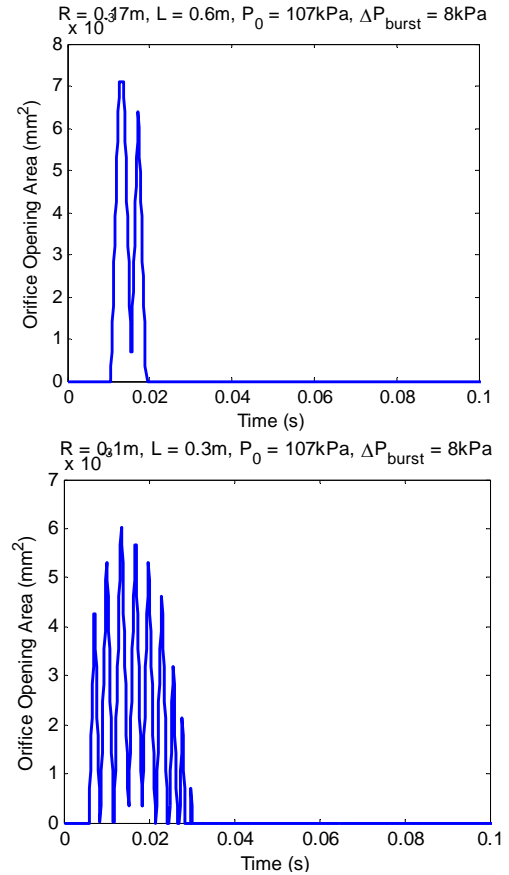


**Figure 8 - Comparison of Orifice Opening Area under Different Airbag Geometries (TOP). Airbag of Radius 0.17m and Length 0.6m (BOTTOM). Airbag of Radius 0.1m and Length 0.3m**

Additionally, an important implication of this finding is that the noise content within a design space affects how the sensitivity analysis is performed. This is because the results of the analysis are dependent on how much noise is captured by the choice of step size when performing a finite difference approximation to a derivative in the design space. This is addressed in the next section.

### System Sensitivities

As a result of the findings made in the first part of Section III.A.4, only the sensitivities of the system objective with respect to the design variables have been explored in this study. This is due to the fact that there is currently low confidence in the ability of the model to predict the optimal airbag geometry due to inaccuracies present in the shape function used. Given this, calculating the sensitivities within the system to changes in the lower bounding values at the optimal solution would provide no physical insight into the behavior of the system.

Thus, the sensitivities of the system objective with respect to the design variables were obtained by calculating the normalized gradient vector at the achieved local optimum. Due to the numerical form of the objective function, a forward difference method was used to identify the derivatives of the objective with respect to each design variable. The selection of a forward difference scheme was based on the fact that the lower boundaries of three of the four design variables are active under the SQP optimization result. A central or backward difference scheme would result in a step into an infeasible design domain.

Additionally, the selection of the magnitude of the step change in each design variable took into consideration the noisy nature of the design space. Here, these values were chosen such that they were large enough to avoid the high frequency noise present in the design space, while small enough to fulfill the finite difference accuracy requirement. The chosen step lengths are listed as follows:

**Table 8 – Step Length Selections for Sensitivity Analysis**

Design Variable	Radius	Length	Bag Pressure	Burst Pressure
Step Change	$10^{-3}$	$10^{-3}$	$10^{-3}$	$10^{-3}$

Given the information listed above, the sensitivity of the objective function to each variable was calculated as follows:

$$\nabla \bar{J} = \frac{x^0}{J(x^0)} \nabla J = \frac{x^0}{J(x^0)} \left[ \frac{\partial J}{\partial R} \quad \frac{\partial J}{\partial L} \quad \frac{\partial J}{\partial P_{bagI}} \quad \frac{\partial J}{\partial P_{burst}} \right]^T = [0.986 \quad 1.738 \quad 1.289 \quad 0]^T \quad (7)$$

This result agrees with those previously observed, in that a decrease in airbag radius and length results in a lower Brinkley DRI. Additionally it is also seen that increasing the length of the airbag results in increasing the Brinkley Index by almost a factor of two, when compared to the effects of increasing the radius. This implies that modifying the radius has the strongest effect in terms of improving impact attenuation performance amongst all of the design variables.

### 3.2 Multi-Objective Optimization

In addition to the previously discussed single objective optimization, a multi-objective optimization study was also performed. Here, the additional objective of minimizing system mass was included into the problem formulation. Specifically, the system mass included the mass of the airbag, as well as the mass of the gas internal to it. Hence with this, the problem formulation became:

Minimize  $\beta$  = Maximum injury risk = Maximum Brinkley Direct Response Index & Minimize System Mass

Subject to:

$$\begin{aligned} 0.1 &\leq R \leq 0.5 && [\text{m}] \\ 0.3 &\leq L \leq 0.85 && [\text{m}] \\ P_{bagI} &\geq 101325 && [\text{Pa}] \\ \Delta P_{burst} &\geq 0 && [\text{Pa}] \end{aligned}$$

In order to solve this multi-objective problem, a full factorial expansion over the objective space was performed. The choice of this method came after a series of experiments with the Multi-Objective Genetic Algorithm, where significant issues with clustering of Pareto points and significantly long computation times were observed. The result of this is presented in Figure 10.

Here, it can be observed that moving along the Pareto front corresponds to varying the valve burst pressure at the minimum airbag geometry such that bottoming-out does not occur. It is important to note that this trend was directly driven by the choice of the valve concept implemented within the system, and that it would most likely change if the characteristics of the valve were made variable.

Upon observation of Figure 10, the trends found in the single objective optimization can be seen to again hold true. In particular, this refers to the fact that at constant burst pressures, the objectives are mutually supporting. This in turn reflects the trend that smaller geometries (and hence lower masses) result in lower Brinkley DRI values, and hence improved impact attenuation. Moreover, it was found that the lower bounds at each of these constant burst pressure values corresponded to the minimum geometry such that bottoming-out of the system did not occur. The fact that these points also corresponded to the Pareto points within the objective space agrees with the conclusions made in Section III.A.4. This also explains the concave shape of the Pareto front, in that the non-dominant solutions along mutually opposing sets of objectives results in solutions being close to equidistant from the utopia point.

Furthermore, it is interesting to note that the observations discussed here would not have been so easily made if a full factorial method was not used, thus reinforcing the value of being able to visualize the relationship between both non-dominated and dominated design solutions.

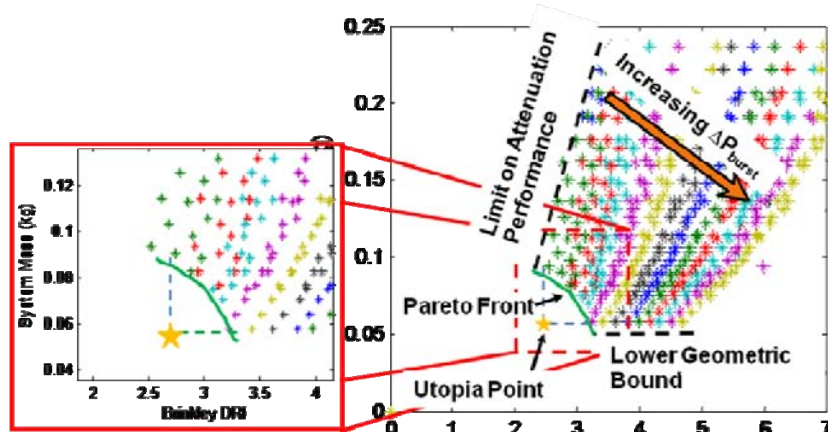


**Figure 10 – Full Factorial Expansion of the Objective Space. Design points of the same color correspond to those with the same burst pressure**

#### IV. Conclusion

A simplified version of a multi-airbag alternative impact attenuation system was modeled and used as the basis of both a single and multi- objective optimization study. From this, it was found that when pressure relief valves are selected as the system’s venting mechanism; two opposing factors influence its geometry. The first is driven by the operation of the valve itself, where smaller geometries are desired to maintain higher pressures over longer periods of time. This in turn causes the venting orifice to remain open for longer, thus allowing more gas and hence energy to be removed from the system. Contrastingly, the second factor is related to the cushioning effect of airbags, whereby larger airbag geometries are desired to avoid a phenomenon known as bottoming-out. This is where the system occupant makes direct contact with the ground. From this, it was found that the best performing airbag systems, in terms of both impact attenuation performance and mass efficiency; were those that had the smallest geometry such that bottoming-out did not occur. Changing the burst pressure while maintaining these conditions corresponded to moving along the Pareto front between mass and Brinkley Index.

In addition, when calculated over the feasible design space, the Brinkley Index was found to contain low amplitude, high frequency noise content due to the iterative manner in which it is calculated. This noise in turn caused a slight discrepancy in the trends observed between gradient-based and heuristic optimization methods; and also influenced how the sensitivity analysis was performed.

With this knowledge, a multi-airbag system will be composed and implemented into the existing multi-disciplinary system design optimization framework in the near future, thereby allowing a more informed system design to be performed. This will in turn significantly contribute towards potentially bringing significant mass-savings to current and future manned spacecraft systems.

#### Acknowledgments

The authors would like to thank Professors Olivier de Weck and Karen Willcox, Dr Anas Alfaris, as well as Andrew March and Kaushik Sinha for their guidance and tutelage during the Spring 2010 16.888 Multidisciplinary System Design Optimization Class.

#### References

<sup>1</sup>de Weck, O.L, “Personal Airbag System – NASA NESC Research Project Overview,” Presentation to NESC Orion Alternative Seat Attenuation Systems Team, March 17 2009  
<sup>2</sup>NASA Constellation Program Human-Systems Integration Requirements, CxP 70024, Released 15 December, 2006  
<sup>3</sup>Cole, J.K. and Wayne, D.E., “BAG: A Code for Predicting the Performance of a Gas Bag Impact Attenuation System for the PATHFINDER Lander,” SAND93-2133, November 1993

MIT OpenCourseWare  
<http://ocw.mit.edu>

ESD.77 / 16.888 Multidisciplinary System Design Optimization  
Spring 2010

For information about citing these materials or our Terms of Use, visit: <http://ocw.mit.edu/terms>.